J|A|C|S

A R T I C L E S

Dimethyl- and Bis[(trimethylsilyl)methyl]cuprates Show Aggregates Higher than Dimers in Diethyl Ether: Molecular Diffusion Studies by PFG NMR and Aggregation−Reactivity Correlations

Xiulan Xie,[†] Carsten Auel,[†] Wolfram Henze,[‡] and Ruth M. Gschwind*,[‡]

Contribution from the [†]Fachbereich Chemie, Philipps-Universität Marburg, Hans-Meerwein-Strasse, D-35032 Marburg, Germany and [‡]Kekulé-Institut für Organische Chemie und Biochemie, Rheinische Friedrichs-Wilhelms-Universität Bonn, Gerhard-Domagk-Strasse 1, D-53121 Bonn, Germany

Received March 25, 2002 ; E-mail: gschwind@uni-bonn.de

Abstract: The molecular sizes of higher aggregates of dimethylcuprates (Me$_2$CuLi (**1**), **1**·LiI, and **1**·LiCN) and bis[(trimethylsilyl)methyl]cuprates ((Me$_3$SiCH$_2$)$_2$CuLi (**2**), **2**·LiI, and **2**·LiCN) in diethyl ether (Et$_2$O) were determined by pulsed field gradient (PFG) NMR diffusion measurements. The obtained diffusion coefficients show molecular sizes larger than those of dimers for all systems. In these higher aggregates, steric hindrance and dilution reduce aggregation, whereas LiCN increases it. The molecular sizes were first determined by a spherical model-free approach and then refined by structure models of higher aggregates. These models were built by a combination of diffusion results, known NMR studies, and crystal structures. Thus, polymeric chains with homodimeric cores connected by solvent (salt-free case) or solvent and salt (salt-containing case) were proposed. These models were confirmed by a solvation analysis, whereby the number of solvent molecules attached to the aggregates was determined by a weighted average study. On the basis of these structure models, the number of repetition units (length index) was determined to be between 1.3 and 5.2, with the general trends in aggregation independent of the structure model used. A combined analysis of the determined length indices and known relative reactivities led for the first time to a correlation between higher aggregation and reactivity of dimethylcuprates in the addition reaction with enones: aggregates higher than dimers reduce the reactivity. Consequently, despite their consistent homodimeric core structures, for the first time the remaining reactivity differences between iodo- and cyanodimethylcuprates in Et$_2$O are explained by the difference in their aggregation.

Introduction

Organocuprates are one of the most frequently applied transition metal reagents for the formation of C−C bonds in the synthetic community.[1−3] Despite their wide application, the structures of these reagents in solution are not fully determined yet.[4,5] Especially, reports of different reactivities for cyano- and iodocuprates led to a long-standing scientific discussion about the structural reasons for these observations.[4,6−8] The discussion about "lower order" or "higher order" cuprates has been decided in favor of the "lower order" cuprates, thus determining the monomeric units of dialkylcuprates to be Gilman cuprates.[4,6,8] In the course of these structural investigations, heterodimeric

and homodimeric structures were proposed for salt-containing and salt-free dialkylcuprates in diethyl ether (Et$_2$O), respectively (for overview, see references in Gschwind et al.[9]). However, our recent investigations based on NOE studies of Me$_2$CuLi (**1**) and Me$_2$CuLi·LiCN (**1**·LiCN) in Et$_2$O showed that also salt-containing dimethylcuprates prefer homodimeric core units in Et$_2$O.[9] In contrast to this uniform homodimeric core structure, comparisons of relative reactivities from logarithmic reactivity profiles (LRPs) of **1**·LiCN and **1**·LiI in Et$_2$O show differences for these two compounds.[10] This led to the question of whether there exists any structural explanation for these reactivity differences. One clue was given by NOE investigations of dimethylcuprates, where negative ^{1}H, ^{1}H NOEs were observed. This negative sign indicates aggregates higher than dimers (hereafter referred to as higher aggregates) in Et$_2$O.[9] Additionally, earlier studies in solution by ^{15}N NMR spectroscopy[11] and electrospray ionization mass spectrometry[12] provided further

---

[†] Philipps-Universität Marburg.
[‡] Rheinische Friedrichs-Wilhelms-Universität Bonn.
(1) Lipshutz, B. H. *Organometallics in Synthesis*; Schlosser, M., Ed.; Wiley: Chichester, U. K., 1994; pp 283−382.
(2) *Organocopper Reagents: A Practical Approach*; Taylor, R. J. K., Ed.; Oxford University Press: Oxford, U. K., 1994.
(3) Krause, N. *Metallorganische Chemie*; Spektrum Akademischer Verlag: Heidelberg, Germany, 1996; pp 175−191.
(4) Krause, N. *Angew. Chem.* **1999**, *111*, 83−85.
(5) Nakamura, E.; Mori, S. *Angew. Chem.* **2000**, *112*, 3902−3924.
(6) Bertz, S. H. *J. Am. Chem. Soc.* **1990**, *112*, 4031−4032.
(7) Lipshutz, B. H.; Sharma, S.; Ellsworth, E. L. *J. Am. Chem. Soc.* **1990**, *112*, 4032−4034.
(8) Bertz, S. H. *J. Am. Chem. Soc.* **1991**, *113*, 5470−5471.

(9) Gschwind, R. M.; Xie, X.; Rajamohanan, P. R.; Auel, C.; Boche, G. *J. Am. Chem. Soc.* **2001**, *123*, 7299−7304.
(10) Bertz, S. H.; Chopra, A.; Eriksson, M.; Ogle, C. A.; Seagle, P. *Chem.−Eur. J.* **1999**, *5*, 2680−2691.
(11) Bertz, S. H.; Nilsson, K.; Davidson, Ö.; Snyder, J. P. *Angew. Chem.* **1998**, *110*, 327−331.
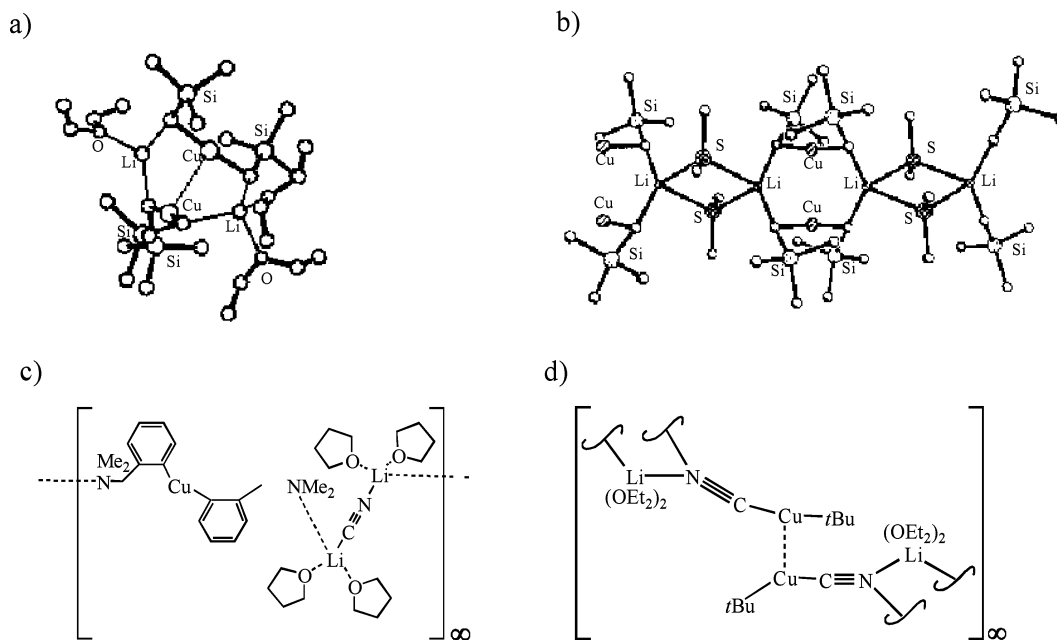
a)

b)

c)

d)

Figure 1. Crystal structures of (a) [Li$_2$Cu$_2$(CH$_2$SiMe$_3$)$_4$(Et$_2$O)$_3$][13] and (b) [Li$_2$Cu$_2$(CH$_2$SiMe$_3$)$_4$(SMe$_2$)$_2$]$_\infty$;[14] structure schemes of (c) [{2-(Me$_2$NCH$_2$)C$_6$H$_4$}$_2$-CuLi$_2$(CN)(THF)$_4$]$_\infty$[15] and (d) [*t*-BuCu(CN)Li(OEt$_2$)$_2$]$_\infty$.[16]

indications for higher aggregates. In the meanwhile, also crystal structures of dialkylcuprates had been determined, showing dimers as well as polymeric chains (Figure 1a, b).[13,14] Examples for polymeric chain structures were also revealed in a diaryl-cyanocuprate and a heteroleptic cuprate (Figure 1c, d).[15,16] Thus, the different aggregation of homodimeric core units in solution seemed to be a possible explanation for the differences in reactivities and therefore a promising starting point for further structure investigations.
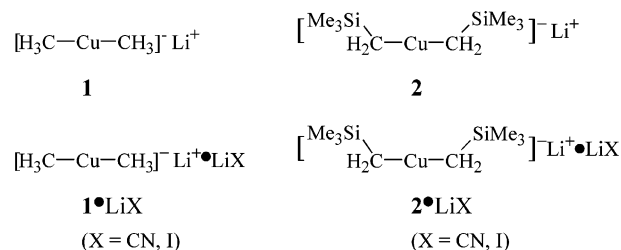
Pulsed field gradient (PFG) diffusion NMR experiments[17,18] offer a powerful tool to investigate the molecular size of these aggregates in solution. Some recent publications verified that diffusion measurements by PFG NMR are also applicable to organometallic compounds.[19−22] Keresztes and Williard even showed that, in the case of organolithium compounds, directly attached solvent molecules have to be included in the calculation of the diffusion coefficient.[21]

In this paper, we present a detailed study of molecular size and possible aggregation structures of dialkylcuprates in Et$_2$O by PFG NMR diffusion experiments. Several structure models for dialkylcuprates with and without salt were proposed and confirmed by solvation analysis. With these structure models as well as a spherical model-free approach, the sizes of the

aggregates were determined and the influence of salt, steric hindrance, and concentration on the aggregation was investigated. Furthermore, for the first time a correlation between reactivity and aggregation state of dimethylcuprates in Et$_2$O is presented.

Results and Discussion

Analysis of Diffusion Coefficients. In general, the signal attenuation in PFG NMR diffusion experiments can be described by the Stejskal−Tanner equation and is presented as Stejskal−Tanner plots.[21,23,24] In these plots, the slope of the signal attenuation represents the diffusion coefficient:[24] the less the attenuation, the lower the diffusion coefficient, the larger the molecular size. For the diffusion studies presented, two model systems with different steric hindrances were used: Me$_2$CuLi (**1**) and (Me$_3$SiCH$_2$)$_2$CuLi (**2**); the salt effect on aggregation was investigated by using salt-free (**1**, **2**) and salt-containing samples (**1·LiI**, **1·LiCN**, **2·LiI**, and **2·LiCN**).

$$[\text{H}_3\text{C}-\text{Cu}-\text{CH}_3]^-\ \text{Li}^+$$

1

$$\left[\begin{smallmatrix}\text{Me}_3\text{Si}\\ \text{H}_2\text{C}\end{smallmatrix}\text{C}-\text{Cu}-\text{C}\begin{smallmatrix}\text{SiMe}_3\\ \text{H}_2\end{smallmatrix}\right]^-\ \text{Li}^+$$

2

$$[\text{H}_3\text{C}-\text{Cu}-\text{CH}_3]^-\ \text{Li}^+\!\bullet\text{LiX}$$

1•LiX

(X = CN, I)

$$\left[\begin{smallmatrix}\text{Me}_3\text{Si}\\ \text{H}_2\text{C}\end{smallmatrix}\text{C}-\text{Cu}-\text{C}\begin{smallmatrix}\text{SiMe}_3\\ \text{H}_2\end{smallmatrix}\right]^-\ \text{Li}^+\!\bullet\text{LiX}$$

2•LiX

(X = CN, I)

The respective Stejskal−Tanner plots obtained by ^{1}H PFG double-stimulated-echo (DSE) experiments[23] are shown in

(12) Lipshutz, B. H.; Keith, J.; Buzard, D. J. *Organometallics* **1999**, *18*, 1571−1574.
(13) John, M.; Auel, C.; Behrens, C.; Marsch, M.; Harms, K.; Bosold, F.; Gschwind, R. M.; Rajamohanan, P. R.; Boche, G. *Chem.−Eur. J.* **2000**, *6*, 3060−3068.
(14) Olmstead, M. M.; Power, P. P. *Organometallics* **1990**, *9*, 1720−1722.
(15) Kronenburg, C. M. P.; Jastrzebski, J. T. B. H.; Spek, A. L.; van Koten, G. *J. Am. Chem. Soc.* **1998**, *120*, 9688−9689.
(16) Boche, G.; Bosold, F.; Marsch, M.; Harms, K. *Angew. Chem.* **1998**, *110*, 1779−1781; *Angew. Chem., Int. Ed. Engl.* **1998**, *1737*, 1684−1686.
(17) Tanner, J. E. *J. Chem. Phys.* **1970**, *52*, 2523−2526.
(18) Johnson, C. S., Jr. *Prog. Nucl. Magn. Reson. Spectrosc.* **1999**, *34*, 203−256.
(19) Valentini, M.; Pregosin, P. S.; Ruegger, H. *Organometallics* **2000**, *19*, 2551−2555.
(20) Jiang, Q.; Ruegger, H.; Venanzi, L. M. *Inorg. Chim. Acta* **1999**, *290*, 64−79.
(21) Keresztes, I.; Williard, P. G. *J. Am. Chem. Soc.* **2000**, *122*, 10228−10229.
(22) Schlörer, N. E.; Berger, S. *Organometallics* **2001**, *20*, 1703−1704.

(23) Jerschow, A.; Müller, N. *J. Magn. Reson.* **1997**, *125*, 372−375.
(24) Stejskal−Tanner equation: $\ln(I/I_0) = -[\gamma^2\delta^2 G^2(\Delta-\delta/3)]D$, where I is the signal intensity, I_0 is the signal intensity in the absence of gradients, γ is the magnetogyric ratio of the observed nucleus, δ is the gradient duration, G is the gradient strength, and Δ is the diffusion delay. Stejskal−Tanner plot: x axis = $[\gamma^2\delta^2 G^2(\Delta-\delta/3)]$; y axis = $\ln(I/I_0)$. Thus, by linear least-squares fitting of the experimental data presented in a Stejskal−Tanner plot to the Stejskal−Tanner equation, the diffusion coefficient D can be obtained.
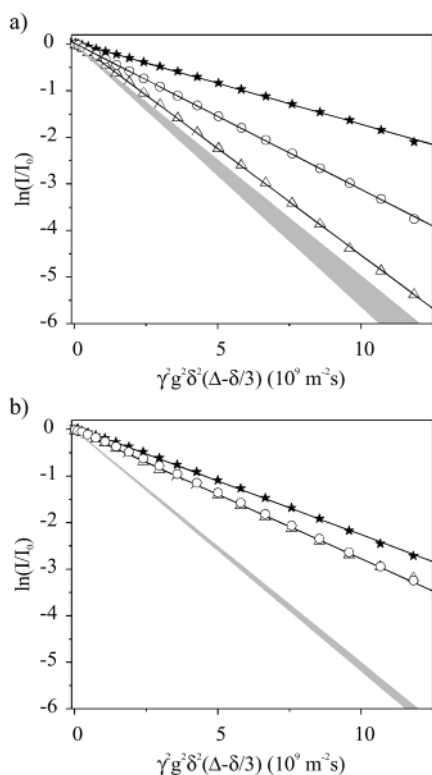
Figure 2. Stejskal−Tanner plots from ^{1}H PFG DSE diffusion experiments in Et₂O at 239 K of (a) bis[(trimethylsilyl)methyl] and (b) dimethyl-cuprates: (a) **2** (△), **2**·LiI (○), and **2**·LiCN (★) and (b) **1** (△), **1**·LiI (○), and **1**·LiCN (★). The solid lines represent linear least-squares fits to the experimental data. The theoretical attenuation ranges for dimers are shown in gray.

Table 1. Diffusion Coefficients D (10^{-9} m² s⁻¹), Molecular Radii r_c (10^{-10} M),[a] Length Indices n and n_{mf}, Solvation Indices n_{solv}, and Theoretical Solvation Indices $n_{solv(t)}$ of Organocuprates in Et₂O at 239 K

complex	$r_c{}^{a,c}$	D	$n_{mf}{}^b$	n^c	n_{solv}	$n_{solv(t)}{}^c$
(Me₃SiCH₂)₂CuLi	5.39	0.59	1.3	1.7	4.8	3.2
(Me₃SiCH₂)₂CuLi·LiI	6.05	0.54	1.1	1.4	7.5	5.4
	(6.39)			(1.3)		(7.5)
(Me₃SiCH₂)₂CuLi·LiCN	6.01	0.35	4.5	3.6	6.9	4.6
	(6.35)			(3.2)		(6.6)
Me₂CuLi	4.22	0.53	4.4	3.1	2.4	2.6
Me₂CuLi·LiI	5.20	0.51	2.2	2.3	6.3	4.9
	(5.64)			(1.9)		(7.0)
Me₂CuLi·LiCN	5.14	0.33	9.0	5.2	5.1	4.4
	(5.58)			(4.5)		(6.4)

[a] r_c = radius of the core units calculated by molecular hard-sphere volume increments. [b] n_{mf} is the aggregation number calculated by a model-free approach (see text for details). [c] For salt-containing complexes, two sets of values are given: those obtained from model C (without brackets) and from model D (in brackets).

less hindered dimethyl sulfide (Me₂S) results in a change from homodimers to polymeric chains.

Structure Models and Determination of Length Indices *n*. Is it now possible to determine structural details of these higher aggregates in solution? In principle, from diffusion measurements only hydrodynamic radii can be obtained. Therefore, we present as one approach aggregation data based solely on the experimentally determined number of solvents and a spherical shape (hereafter referred to as model-free approach). Additionally and more interestingly, in the case of dialkyl-cuprates we can combine several independent sources of information for the construction of structure models for higher aggregates. These comprise NOE studies,[9] crystal structures,[13−16] as well as the salt dependence of the aggregates and involvement of solvent molecules in aggregation presented in this study. On the basis of these models, a second refined set of aggregation data is presented.

First, we discuss the structure model for higher aggregates of salt-free dialkylcuprates. In this case, homodimeric core structures have been verified by various theoretical as well as experimental results.[5,9,13,14,27,28] Furthermore, recently we showed by ^{1}H, [6]Li HOE studies the analogy between the homodimeric core structures in the solid state and those in solution.[9] If they are connected through solvent molecules, these homodimers can form higher aggregates, a straightforward model, which is sup-ported by the crystal structure of [Li₂Cu₂(CH₂SiMe₃)₄(SMe₂)₂]∞[14] (Figure 1b). Thus, our model for salt-free dialkylcuprates comprises a polymeric chain with homodimeric core structures bridged by solvent molecules: model A (Figure 3a).

For salt-containing dialkylcuprates, the situation is more complicated because of the additional structural possibilities to array Li−X (X = I⁻, CN⁻). One probable arrangement comprising heterodimeric core structures is shown in Figure 3b, where heterodimers are linked by solvent molecules: model B. However, a heterodimeric model is not in agreement with the dependence of the diffusion coefficients on the kind of salt discussed previously. If heterodimeric core structures existed, the salt molecules would be part of the heterodimer and only solvent molecules would remain as bridging units. Then, the

Figure 2. The theoretical attenuation ranges of the respective dimeric structures are indicated in gray.[25] Figure 2 shows that all compounds exhibit a signal attenuation clearly less than that expected for dimers. This indicates higher aggregates of these organocuprates in solution. Additionally, salt effects are ob-served: (1) LiCN causes larger molecular sizes than LiI for both types of cuprates, **1**·LiX, and **2**·LiX; (2) **2**·LiI shows larger aggregates than **2**.

For a quantitative analysis of molecular size, the diffusion coefficients obtained from the diffusion NMR experiments have to be corrected by the intrinsic viscosity of each sample.[26] The viscosity-corrected values of D in Et₂O at 239 K are listed in Table 1 (see Experimental Section for details of viscosity correction). For **2**, **2**·LiI, and **2**·LiCN, the D values are 0.59, 0.54, and 0.35 × 10^{-9} m² s⁻¹, which indicate a trend in the molecular size: **2** < **2**·LiI < **2**·LiCN. For **1**, **1**·LiI, and **1**·LiCN, the D values are 0.53, 0.51, and 0.33 × 10^{-9} m² s⁻¹, showing a similar trend in molecular size. Despite the smaller monomeric unit of **1**, the D values of **1** and **1**·LiX (X = I, CN) are even smaller than the corresponding values of **2** and **2**·LiX. This denotes larger aggregates for **1** and **1**·LiX and can be interpreted as an effect of less steric hindrance in dimethylcuprates. A similar trend was already found in crystal structures (Figure 1a, b), where a replacement of the solvent from Et₂O to the

(25) Theoretical ranges of signal attenuation for dimeric structures were calculated by using the Stejskal−Tanner equation, with diffusion coef-ficients determined according to the Stokes−Einstein theory $D = (kT)/(6\pi\eta r)$: r_{max} = radius of homodimer, r_{min} = radius of heterodimer (see Figure 3a, b with n = 1); k is the Boltzmann constant, T is the absolute temperature, and η is the viscosity of the corresponding salt-free sample.
(26) Cabrita, E. J.; Berger, S. *Magn. Reson. Chem.* **2001**, *39*, 142−148.

(27) Böhme, M.; Frenking, G.; Reetz, M. T. *Organometallics* **1994**, *13*, 4237−4245.
(28) Bertz, S. H.; Vellekoop, A. S.; Smith, R. A. J.; Snyder, J. P. *Organometallics* **1995**, *14*, 1213−1220.
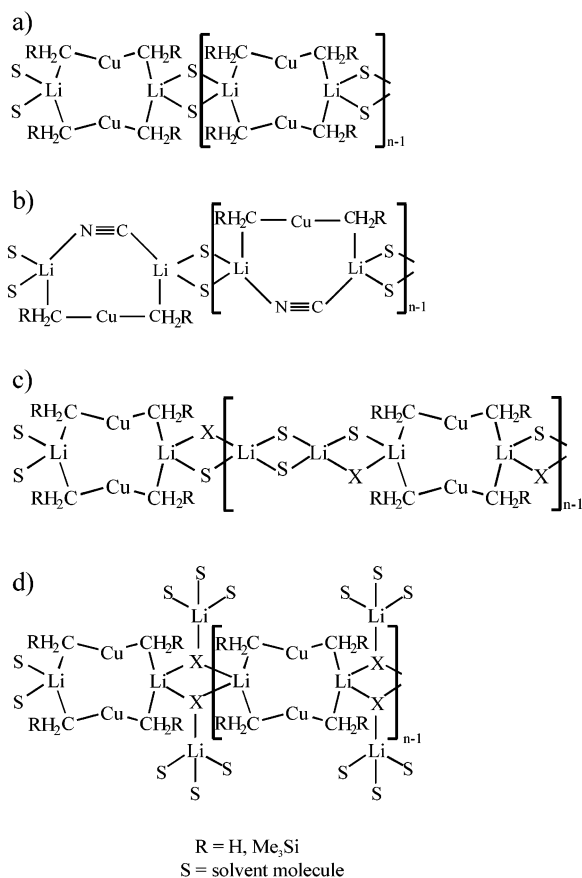
R = H, Me₃Si
S = solvent molecule

Figure 3. Structure models of aggregates higher than dimers: (a) salt-free homodimeric chain (model A), (b) salt-containing heterodimeric chain (model B), (c) and (d) salt-containing homodimeric chains (models C and D).

length of the chain would be almost independent of the kind of salt. This runs contrary to the strong salt dependence observed (Figure 2), and therefore, a heterodimeric model (model B) can be excluded.

The homodimeric models are in agreement with recent experimental results, which show that also salt-containing dialkylcuprates prefer homodimeric core structures in Et₂O.[9] Additionally, the salt dependence of the aggregation indicates an involvement of the salt in the structure of the higher aggregates. On the basis of the homodimeric cores, the salt can contribute only to the bridging units. Furthermore, from ^{15}N NMR studies of Bu₂CuLi·LiCN in Et₂O it was proposed that LiCNLi⁺ units exist in solution.[11] Examples of possible arrangements of Li⁺ and CN⁻ units can be taken from the few existing crystal structures (Figure 1c, d). In these structures, two types of coordination for the CN unit exist: in the crystal structure of [{2-(Me₂NCH₂)C₆H₄}₂CuLi₂(CN)(THF)₄]∞ (Figure 1c),[15] a LiCNLi⁺ unit is realized, while a trigonal arrangement of the CN group with two Li⁺ coordinated to the nitrogen is found in [t-BuCu(CN)Li(OEt₂)₂]∞ (Figure 1d).[16] Thus, two different conjunction arrangements were proposed: model C (Figure 3c) and model D (Figure 3d). They represent two possible salt-bridging arrangements and were both used in the following calculations.

In all cases, by using the model-free approach without structural assumptions as well as the structure models presented, higher aggregation was calculated from the diffusion coefficients. In the model-free approach, the Stokes−Einstein

theory[29] for spherical molecules was used to determine the molecular size. The volumes and the radii of the repetition units were calculated by hard-sphere volume increments[30,31] using the stoichiometric composition. The numbers of solvent molecules attached were determined by solvation analysis (see later text). Thus, the calculated numbers of repetition units, defined as model-free aggregation numbers n_{mf}, are listed in Table l.

In the case of nonspherical molecules, such as our model systems, the Stokes−Einstein theory has to be modified by a shape factor.[32] As a first approximation, all of our structure models were considered to be cylinders composed of spherical repetition units. The radii (r_c) of these repetition units (Figure 3 with $n = 1$) represent the radii of the cylinders. The volumes and the radii of the respective repetition units were calculated by hard-sphere volume increments.[30,31] The lengths of the polymeric chains (the cylinders) reflect the individual aggregate of each sample and can therefore be determined from the measured diffusion coefficients. The chain lengths and thus the length indices n were calculated by an iterative procedure, details of which are described in the Supporting Information. The calculated r_c and n are also listed in Table 1.

For the model-free approach, the aggregation number n_{mf} obtained for the salt-free complexes **1** and **2** are 4.4 and 1.3, while, for the chain structure of the salt-free model A, the length indices n obtained are 3.1 and 1.7, respectively. The reduction in the chain length of **2** compared with **1** can be explained by the less steric hindrance in **1**, a trend that has already been discussed in the analysis of the diffusion coefficients. For the salt-containing complexes, the results of the model-free approach and the structure models C and D have to be considered. First, the two models are discussed. For model C, the calculated n values are 1.4, 3.6, 2.3, and 5.2 for **2**·LiI, **2**·LiCN, **1**·LiI, and **1**·LiCN, while, for structure model D, the corresponding values are 1.3, 3.2, 1.9, and 4.5. Three trends can be recognized in these values: (1) the length index n is generally larger for model C than for model D, which is caused by the smaller repetition unit of model C (C, four solvent molecules; D, six solvent molecules); (2) the n values of **1**·LiX are larger than the corresponding ones of **2**·LiX, which is similar to the salt-free case and can be explained by the less steric hindrance of **1**·LiX; (3) dialkylcuprates containing LiCN show larger n values than those containing LiI, which is in agreement with the expected bridging ability of LiCNLi⁺ > LiILi⁺, according to the HSAB principle.

For the model-free approach, the calculated n_{mf} values are 1.1, 4.5, 2.2, and 9.0 for **2**·LiI, **2**·LiCN, **1**·LiI, and **1**·LiCN. The model independent trends 2 and 3 are again valid, with the salt dependence of aggregation even amplified. The deviations in the absolute values compared with models C and D are caused by two parameters: the shape factor F and the number of solvent molecules attached. For small n, the shape factor is close to 1; thus, mainly the number of solvent molecules causes the deviations. With an increasing value of n, the shape factor gains influence and the deviation in the absolute values increases. A conspicuous example is the high value of 9.0 for **1**·LiCN in

(29) Edward, J. T. *J. Chem. Educ.* **1970**, *47*, 261−270.
(30) Ben-Amotz, D.; Willis, K. G. *J. Phys. Chem.* **1993**, *97*, 7736−7742.
(31) Bondi, A. *J. Phys. Chem.* **1964**, *68*, 441−451.
(32) Bloomfield, V. A. In *On-Line Biophysics Textbook*; Schuster, T. M., Ed.; Separation and Hydrodynamics; Biophysical Society: Bethesda, MD, 2000; pp 1−5. http://www.biophysics.org/biophys/society/btol.
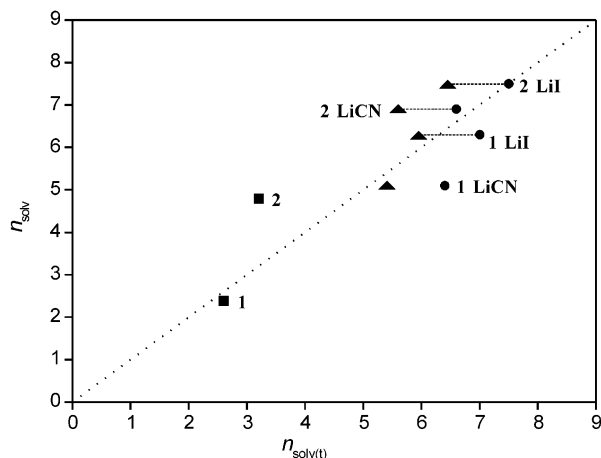
Figure 4. Correlation between the experimental (n_{solv}) and theoretical ($n_{solv(t)}$) solvation number of bis[(trimethylsilyl)methyl]- (**2** and **2**·LiX) and dimethylcuprates (**1** and **1**·LiX) in Et₂O for model A (■), model D (●), and the average of models C and D (▲).

Figure 5. Correlation between aggregation and reactivity of dimethylcuprates in Et₂O. The numbers given are the yields at 4 s out of known LRP data,[10] which are used as an approximation for the different reactivities of the respective dimethylcuprates.

the spherical approach compared with 5.2 and 4.5 for models C and D, which means that higher aggregation is overemphasized by using a spherical model. A detailed table, which reflects the influence of shape factor, is given in the Suppporting Information (Table S1). In general, it can be stated that the absolute values of *n*, especially for higher *n* values, depend on the assumption of a shape or model. However, the important trends for the understanding of reactivities in aggregation are independent of the models used.

Solvation Analysis. As a next step, the solvent involvement in aggregation is discussed. Since solvent molecules contribute to the investigated aggregates, their diffusion coefficient can be used for the model-free approach and as an independent parameter to confirm our proposed structure models. Because of the fast exchange of the solvent molecules, their apparent diffusion coefficient D_{obs} represents a mean value of free solvent molecules and those involved in the aggregation.[33,34] Thus, the number of solvent molecules directly attached to each repetition unit (n_{solv}) was obtained from this weighted average (details of calculation are given in the Supporting Information). The results for n_{solv} are listed in Table 1. The obtained n_{solv} are 2.4, 6.3, and 5.1 for **1**, **1**·LiI, and **1**·LiCN and 4.8, 7.5, and 6.9 for **2**, **2**·LiI, and **2**·LiCN. To compare these experimental solvation numbers n_{solv} with our structure models, ideal solvation numbers for each model ($n_{solv(t)}$) were also calculated (A, $(2n + 2)/n$; C, $(4n + 2)/n$; D, $(6n + 2)/n$; *n*, length index). The obtained $n_{solv(t)}$ (listed in Table 1) are 2.6 and 3.2 for **1** and **2**, respectively. In the case of salt-containing cuprates, $n_{solv(t)}$ depends on the model used. Thus, for model C, the values 4.9, 4.4, 5.4, and 4.6 were obtained for **1**·LiI, **1**·LiCN, **2**·LiI, and **2**·LiCN, while, for model D, the values 7.0, 6.4, 7.5, and 6.6 were obtained for **1**·LiI, **1**·LiCN, **2**·LiI, and **2**·LiCN. For a straightforward interpretation of these data, a graphical correlation between $n_{solv(t)}$ and n_{solv} for models A and D and the average of C and D is given in Figure 4. The diagonal represents an ideal agreement between the two parameters. Correlation points above the diagonal indicate a solvation higher than calculated for the structure models, and those below the diagonal indicate a solvation that
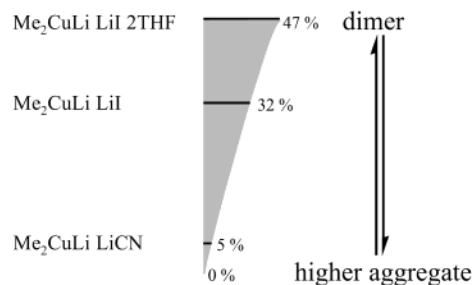
is lower. Most of the data points for **2** and **2**·LiX are above the diagonal line, with a preference of **2**·LiX for model D. This means that model D fits better to **2**·LiX than model C. Most of the data points for **1** and **1**·LiX are below the diagonal line with a preference of **1**·LiX for the average of models C and D. Thus, a possible interpretation for **1**·LiX is that a mixture of models C and D exists in their higher aggregates. The overall agreement between the experimental and the theoretical values of the solvation numbers presented in Figure 4 supports our proposed structure models of higher aggregates of dialkylcuprates.

Concentration Dependence. After the validation of the structure models, the concentration dependence of the aggregation was examined. For this purpose, the diffusion coefficients and the length indices of **1**·LiI and **1**·LiCN at different concentrations were determined. For **1**·LiI at concentrations of 0.76, 0.64, 0.44, and 0.24 M, length indices for model C of 2.3, 1.8, 1.5, and 1.2 were obtained. For **1**·LiCN at concentrations of 0.78, 0.58, and 0.48 M, length indices for model C of 5.2, 3.9, and 3.7 were derived. As expected, the aggregation of dialkylcuprates shows a significant dependence on the sample concentration. This trend is independent from the model used and can be connected with the dependence of aggregation on sterical hindrance and on the kind of salt. Thus, for larger substituents lower aggregation is expected at similar concentrations, whereas a change in the salt from LiI to LiCN causes higher aggregation.

Aggregation–Reactivity Correlation. The elucidation and quantification of higher aggregates of dialkylcuprates in Et₂O enabled us to tackle the most interesting question: how does higher aggregation influence the reactivity of cuprates? Recently we showed that in the addition reaction with enones the reactivity of cuprates increases with a change from mainly solvent separated ion pairs in THF to contact ion pairs in Et₂O.[13] Thus, likewise an influence on the reactivity due to a change from homodimer to oligomer is expected. With the knowledge of higher aggregation from our diffusion studies and known relative reactivities, a first correlation between reactivity and higher aggregation can be established. Kinetic data for **1**·LiI in Et₂O were published by Casinius et al.[35] Relative reactivities were presented by Bertz et al.,[10] which can be used to show higher aggregation caused by different salts. In this second publication, relative reactivities from LRPs are presented for many organocuprates with various conditions; among them are **1**·LiI·2THF, **1**·LiI, and **1**·LiCN at 0.1 M in Et₂O. As acceptable

(33) Böckmann, A.; Guittet, E. *FEBS Lett.* **1997**, *418*, 127−130.
(34) Price, W. S.; Tsuchiya, F.; Arata, Y. *J. Am. Chem. Soc.* **1999**, *121*, 11503−11512.

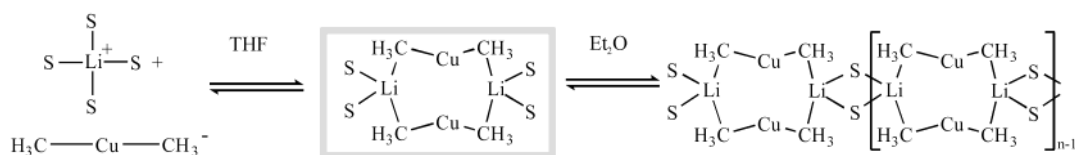(35) Canisius, J.; Gerold, A.; Krause, N. *Angew. Chem.* **1999**, *111*, 1727−1730.

Figure 6. Equilibria between different aggregation states of dimethylcuprates in etheral solvents. The reactive dimer is highlighted by a gray frame.

approximations of the different reactivities, the yields at 4 s were used, which are 47%, 32%, and 5.3% for **1·LiI·2THF**, **1·LiI**, and **1·LiCN**.[10] These numbers show clearly that **1·LiI·2THF** is the most reactive one among these three; the next reactive is **1·LiI**, and far the least reactive is **1·LiCN**. A close inspection of the absolute numbers show that the difference between **1·LiI** and **1·LiCN** is nearly double as large as the difference between **1·LiI·2THF** and **1·LiI**.

To understand the correlation between reactivity and aggregation, as the next step, the aggregation states of these three organocuprates have to be compared with each other. For **1·LiI**, the results of the concentration dependence investigations can be taken, where an aggregate a little bit larger than a dimer ($n = 1.2$) was revealed at 0.24 M. For **1·LiI·2THF**, it is known from the monomer−dimer equilibrium in THF[36] that THF molecules induce deaggregation until there are mainly solvent separated ion pairs in pure THF. Since in **1·LiI·2THF** only two THF molecules are available for each Li^+, only deaggregation to the pure homodimer ($n = 1$) is expected. In **1·LiCN**, however, the higher bridging capability of CN^- leads to length indices more than double compared with **1·LiI** (see Table 1 and concentration dependence). That means there is a considerable difference in aggregation between **1·LiCN** and **1·LiI**, whereas the difference between the nearly dimeric **1·LiI** and the dimeric **1·LiI·2THF** is much less. These aggregation differences reflect directly the reactivity pattern found for the three compounds (see Figure 5), which leads to the conclusion that aggregates higher than dimers reduce the reactivity.

With this aggregation−reactivity correlation, we may understand to some extent the long-standing discussion of whether LiCN-containing cuprates exhibit higher reactivities or not.[10] Recent HOE studies[13,36] and now the presented diffusion studies show that in etheral solvents aggregation plays a dominant role in non-Lewis acid catalyzed addition reactions to enones. In THF, an equilibrium between monomers and dimers was found,[36] whereas, in Et_2O, an equilibrium between dimers and higher aggregates is shown (see Figure 6). The comparison with known relative reactivities shows for both solvents that the dimer is the reactive species for dimethylcuprates in the addition reaction to enones. Formation of higher aggregates in Et_2O as well as deaggregation to monomers in THF[36] leads to a reduction in reactivity. Therefore, the tuning of organocuprate reagents to the dimeric form should enhance their reactivities. To confirm this correlation, diffusion and reactivity studies for various organocuprates are in preparation.

Conclusion

For the first time, aggregates higher than dimers were defined for dialkylcuprates in Et_2O by PFG NMR diffusion measurements. This was demonstrated by salt-free and salt-containing samples of dimethyl- and bis[(trimethylsilyl)methyl]cuprates.

Diffusion coefficients show molecular sizes larger than dimers, and the aggregation extent depends on steric hindrance, salt effects, and sample concentration. Steric hindrance as well as low concentration decreases, whereas salt, especially LiCN, increases aggregation. For the quantitative analysis, first, a spherical model-free approach was used. This approach is based solely on the experimentally determined number of solvents and a spherical shape. The number of aggregations was further refined by structure models, which were built by a combination of known NOE studies, crystal structures, as well as results from current diffusion measurements. These models comprise homo-dimeric cores, which are connected by solvent molecules (salt-free cases) or by bridging units comprising salt and solvents (salt-containing cases). An analysis of the solvation extent of these aggregates confirmed the proposed structure models. A comparison of the different approaches show the general trends being independent of the models used. The absolute n values for small oligomers agree quite well, whereas for larger oligomers the spherical approach even overemphasizes higher aggregation. A combination of the presented aggregation numbers with known relative reactivities shows that for dimethylcuprates mainly the dimer is the reactive species and higher aggregation as well as lower aggregation reduces their reactivity in the addition reaction to enones. Together with the determined salt and concentration dependence, the aggregation of dimethylcuprates can now be tuned to the conditions required for the respective syntheses. Therefore, the presented results can serve as an information source for the manipulation of the reaction system and for a reactivity optimization.

Experimental Section

Sample Preparation. All samples were prepared according to a method described by John et al.[13] A mixed solvent of 80% Et_2O-d_{10} and 20% Et_2O was used for all samples and is denoted as pure Et_2O solvent throughout this paper. The new concentrations were determined by comparing the integrals of the proton spectra obtained by a single 90° pulse with those of the Bruker standard sample 0.1 M urea and 0.1 M methanol in deuterated DMSO at 298 K. Sample concentrations are 0.72, 0.76, and 0.78 M for **1**, **1·LiI**, and **1·LiCN** and 0.60, 0.56, and 0.66 for **2**, **2·LiI**, and **2·LiCN**.

Determination of Diffusion Coeffficients. The diffusion coefficients were determined by linear least-squares fits[37] to the Stejskal−Tanner plots (Figure 2). The obtained diffusion coefficient D_{vis} are 0.42, 0.34, and 0.18×10^{-9} m^2 s^{-1} for **2**, **2·LiI**, and **2·LiCN** and 0.29, 0.28, and 0.20×10^{-9} m^2 s^{-1} for **1**, **1·LiI**, and **1·LiCN**. These are the average results of 3−5 repetitions of each measurement with the following experimental errors: 6% (**1**), 4% (**1·LiI**), 5% (**1·LiCN**), 2% (**2**), 3% (**2·LiI**), and 6% (**2·LiCN**).

Internal Viscosity Reference. The viscosity value of nondeuterated Et_2O at 239 K was obtained by nonlinear fitting to literature data in the temperature range of 173−298 K.[38] The viscosity value of the mixed

(36) Gschwind, R. M.; Rajamohanan, P. R.; John, M.; Boche, G. *Organometallics* **2000**, *19*, 2868−2873.

(37) Linear least-squares fits were carried out by Origin 6.0, Microcal Software Inc.: Northampton, MA 01060, USA.

(38) In *Handbook of Chemistry and Physics*; Hodgman, C. D., Ed.; the Chemical Rubber Publishing Company: Cleveland, OH, 1963; p 2260.

solvent (80% Et_2O-d_{10}/20% Et_2O) used in this study was defined to be 1.1 times the value of the nondeuterated Et_2O at the same temperature.[39,40]

Since we noticed a strong dependence of the viscosity on the concentration and the kind of cuprates, internal references were used for viscosity corrections:[26] a trace (2−3 drops) of Me_4Si for **1** and of C_6H_6 for the left. To check influences of the viscosity references on the cuprate samples, diffusion measurements were performed before and after the addition of the internal viscosity reference. The respective Stejskal−Tanner plots showed no attenuation difference and thus excluded any influence of the viscosity reference. By a comparison of the diffusion coefficients of the reference molecules measured in (1) reference + Et_2O (η) and (2) reference + cuprate + Et_2O (η_{cup}), viscosity correction factors η_{cup}/η for the cuprate samples were determined. The factors are 1.40, 1.60, and 1.95 for **2**, **2·LiI**, and **2·LiCN** and 1.84, 1.82, and 1.67 for **1**, **1·LiI**, and **1·LiCN**. The diffusion coefficients listed in Table 1 were corrected by the respective viscosity correction factors: $D = D_{vis}(\eta_{cup}/\eta)$.

NMR Data Collection and Processing. The NMR spectra were recorded on a Bruker DRX500 spectrometer equipped with a 5 mm broadband triple resonance *Z*-gradient probe (maximum gradient strength 53.5 G/cm). The shape of the gradients was rectangular, with a length of 2 ms, and the strength was varied in 20 increments (5−95%) of the gradient ramp created by Bruker software DOSY. Thus, all diffusion measurements were performed in pseudo 2D mode and processed with Bruker software package t1/t2. For each experiment, 16 dummy scans and 16 scans were used, with a relaxation delay of 6 s. All the measurements were carried out at 239 K controlled by a Bruker BVT 3000 temperature unit.

Supporting Information Available: Calculation of the length indices *n* and solvation indices n_{solv} and a table of shape factors for different structure models. This material is available free of charge via the Internet at http://pubs.acs.org.

JA026311M

(39) Haupts, U.; Maiti, S.; Schwille, P.; Webb, W. W. *Proc. Natl. Acad. Sci. U.S.A.* **1998**, *95*, 13573−13578.
(40) Su, Q.; Klinman, J. P. *Biochemistry* **1999**, *38*, 8572−8581.